

# Strong Kleinman-Forbidden Second Harmonic Generation in Chiral Sulfide: $\text{La}_4\text{InSbS}_9$

Hua-Jun Zhao,<sup>†</sup> Yong-Fan Zhang,<sup>‡</sup> and Ling Chen<sup>\*,†</sup>

<sup>†</sup>Key Laboratory of Optoelectronic Materials Chemistry and Physics, Fujian Institute of Research on the Structure of Matter, Chinese Academy of Sciences, Fuzhou, Fujian 350002, People's Republic of China

<sup>‡</sup>Department of Chemistry, Fuzhou University, Fuzhou, Fujian 350002, People's Republic of China

**S** Supporting Information

**ABSTRACT:** A new chiral sulfide family,  $\text{Ln}_4\text{InSbS}_9$  ( $\text{Ln} = \text{La, Pr, Nd}$ ), with its own structure type in space group  $P4_12_12$  or its enantiomorph  $P4_32_12$  has been synthesized by solid-state reaction. Remarkably, the La member shows the strongest Kleinman-forbidden second harmonic generation to date, with an intensity 1.5 times that of commercial  $\text{AgGaS}_2$  at a laser wavelength of 2.05  $\mu\text{m}$ , and exhibits type-I phase-matchable behavior. Density functional theory calculations and ab initio molecular dynamics simulations suggest that lattice vibrations may be responsible for the origin and magnitude of the strong SHG effect.

The prerequisite of a nonlinear optical (NLO) material is that it be crystallographically noncentrosymmetric (NCS). Out of the total 32 point groups, there are 20 NCS point groups, of which the chiral 422 and 622 ones should have null second harmonic generation (SHG) response under the restriction of Kleinman symmetry.<sup>1</sup> Nevertheless, as a result of dispersion, very small Kleinman-forbidden SHG coefficients are observed. For example,  $\alpha\text{-TeO}_2$  with 422 symmetry shows  $d_{14}(1.328 \mu\text{m}) \approx 0.36 \text{ pm/V}$  or  $d_{14}(1.064 \mu\text{m}) \approx 0.61 \text{ pm/V}$ ,<sup>2a-d,h</sup> and  $(\text{K}_3\text{I})[\text{SmB}_{12}(\text{GaS}_4)_3]$  with 622 symmetry exhibits a powder SHG intensity 0.3 times that of potassium dihydrogen phosphate (KDP) at 1.94  $\mu\text{m}$ .<sup>2e</sup> However, violation cases are also found in large-sized single crystals of  $\alpha\text{-SiO}_2$  (32 point group) and  $\text{LiIO}_3$  (6 point group), for which the unexpected  $d_{14}$  values of  $2.6 \times 10^{-3} \text{ pm/V}^{2f}$  and  $0.24 \text{ pm/V}$ ,<sup>2g</sup> respectively, have been observed. It has also been known that when the second harmonic frequency approaches that of the electronic exciton resonance ( $2h\nu \approx E_g$ ), the small Kleinman-forbidden coefficient can become large.<sup>2a,h-1</sup> For example,  $\alpha\text{-TeO}_2$  shows a large Kleinman-forbidden  $d_{14}$  value of  $\sim 4.32 \text{ pm/V}$  at 0.659  $\mu\text{m}$ , which is 10 times larger than that at 1.328  $\mu\text{m}$ , because the second harmonic wavelength (0.33  $\mu\text{m} \approx 3.76 \text{ eV}$ ) is very close to its optical band gap (3.75 eV).<sup>2a,i,m</sup>

The common strategy to predesign a NCS compound is to involve asymmetric building units in the crystal structure, such as  $d^0$  transition-metal cations ( $\text{Ti}^{4+}$ ,  $\text{Nb}^{5+}$ ,  $\text{W}^{6+}$ , etc.) susceptible to second-order Jahn–Teller distortion or p cations with stereochemically active lone-pair electrons ( $\text{Se}^{4+}$ ,  $\text{Te}^{4+}$ ,  $\text{As}^{3+}$ ,  $\text{Sb}^{3+}$ , etc.).<sup>3</sup> We recently realized that in quaternary rare-earth metal/metal/antimony/chalcogenide systems, the  $\text{SbQ}_4$  polyhedron tends to adopt an asymmetric geometry, such as the

dimeric teeter-totter  $\text{Sb}_2\text{S}_6$  polyhedron in  $\text{Ln}_4\text{GaSbS}_9$ ,<sup>4a</sup> the teeter-totter  $\text{SbQ}_4$  ( $\text{Q} = \text{S, Se}$ ) in  $\text{La}_4\text{FeSb}_2\text{Q}_{10}$ ,<sup>4b</sup> and square-pyramidal  $\text{SbS}_5$  in  $\text{Ln}_2\text{Mn}_3\text{Sb}_4\text{S}_{12}$ .<sup>4c</sup> More interestingly, the arrangement of such asymmetric units is crucially affected by the  $\text{MQ}_4$  polyhedron. For example,  $\text{SbQ}_4$  units are eventually arranged in a centrosymmetric structure when linked by  $\text{FeS}_4$  or  $\text{MnS}_6$ <sup>4b,c</sup> but an NCS structure with a strong SHG effect when linked by  $\text{Ga}_2\text{S}_7$ .<sup>4a</sup>

In this communication, we report an unusual chiral quaternary sulfide showing the strongest Kleinman-forbidden NLO response to date. Density functional theory (DFT) calculations and ab initio molecular dynamics (MD) simulations suggest that lattice vibrations may be responsible for its origin and magnitude.

The compounds  $\text{Ln}_4\text{InSbS}_9$  ( $\text{Ln} = \text{La, Pr, Nd}$ ) crystallize in space group  $P4_12_12$  or its enantiomorph  $P4_32_12$  [Table S1 in the Supporting Information (SI)] and are characterized by unusual  $[\text{In}_2\text{Sb}_2\text{S}_{11}^{10-}]_\infty$  infinite helical chains propagating along the  $c$  direction and separated by isolated  $\text{Ln}^{3+}$  cations and discrete  $\text{S}^{2-}$  anions. These chains are further packed around the  $4_1$  helical axes (Figure 1a). Such chains are built from dimeric teeter-totter  $\text{Sb}_2\text{S}_6$  polyhedra and dual-apex-shared  $\text{In}_2\text{S}_7$  tetrahedra (Figure 1b); they are reminiscent of the chains in  $\text{Ln}_4\text{GaSbS}_9$ <sup>4a</sup> but differ in that  $\text{Sb}_2\text{S}_6$  and  $\text{In}_2\text{S}_7$  are arranged around a 2-fold screw axis, which means that neighboring dimers are oriented in opposite directions (Figure 1c), whereas the neighboring  $\text{Sb}_2\text{S}_6$  or  $\text{Ga}_2\text{S}_7$  in  $\text{Ln}_4\text{GaSbS}_9$  are arranged in-phase (Figure S5 in the SI).

The  $\text{SbS}_4$  polyhedron is remarkably distorted as a consequence of the stereochemically active lone-pair electrons of  $\text{Sb}^{3+}$ , with  $\text{Sb}-\text{S}$  bond distances of 2.44–2.91 Å that are comparable to those found in  $\text{Ln}_4\text{GaSbS}_9$  (2.45–2.84 Å),<sup>4a</sup>  $\text{La}_4\text{FeSb}_2\text{Q}_{10}$  (2.46–2.92 Å),<sup>4b</sup> and  $\text{La}_7\text{Sb}_9\text{S}_{24}$  (2.43–3.00 Å).<sup>5</sup> The  $\text{InS}_4$  tetrahedron is less distorted, with  $\text{In}-\text{S}$  distances of 2.45–2.49 Å and  $\text{S}-\text{In}-\text{S}$  angles ranging from 104 to 111°. These are comparable to those in  $\text{CuInS}_2$ .<sup>6</sup>  $\text{La}^{3+}$  cations and isolated  $\text{S}^{2-}$  anions (sulfur atoms S7, S8, S9, and S10) occur between the infinite helical chains. Thus, the formula can be written as  $(\text{La}^{3+})_8([\text{In}_2\text{Sb}_2\text{S}_{11}]^{10-})(\text{S}^{2-})_7$ . The cationic La1 and La2 exhibit normal  $\text{LaS}_6$  trigonal-prismatic coordination, and La3 and La4 are found in  $\text{LaS}_7$  monocapped trigonal prisms with  $\text{La}-\text{S}$  lengths varying from 2.84 to 3.45 Å, comparable to those in  $\gamma\text{-La}_2\text{S}_3$ ,<sup>7</sup>  $\alpha\text{-La}_2\text{S}_3$ ,<sup>8</sup>  $\text{La}_7\text{Sb}_9\text{S}_{24}$ ,<sup>5</sup> and  $\text{La}_4\text{FeSb}_2\text{S}_{10}$ .<sup>4b</sup>

Received: November 20, 2011

Published: January 10, 2012

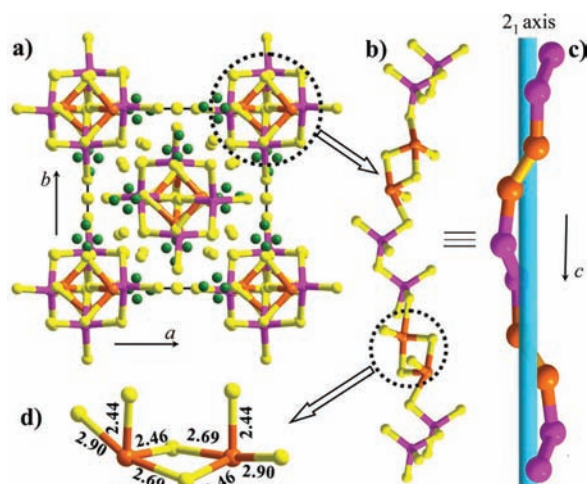


**Figure 1.** (a) View of  $\text{La}_4\text{InSbS}_9$  along (001). (b) Helical  $[\text{In}_2\text{Sb}_2\text{S}_{11}]_{\infty}$  chains along the  $c$  direction. (c) Helical configuration of the chains. S atoms have been omitted for clarity, and the  $2_1$  screw axis is visualized as a thick blue line. (d) Local coordination of the dimeric teeter-totter  $\text{Sb}_2\text{S}_6$  polyhedra. Green, La; pink, In; orange, Sb; yellow, S.

Naturally,  $\text{La}_4\text{InSbS}_9$  is diamagnetic.  $\text{Pr}_4\text{InSbS}_9$  obeys the Curie–Weiss law over the entire experimental temperature region, whereas  $\text{Nd}_4\text{InSbS}_9$  deviates from it below 40 K (Figure S6). Their Curie constants and Weiss temperature are 6.54 and 7.25 emu K/mol and  $-21.67$  and  $-22.74$  K, respectively. The experimental effective magnetic moments are 7.23 and 7.61  $\mu_B$ , respectively, which are comparable to the calculated values, 7.16 and 7.24  $\mu_B$ .<sup>9</sup>

The optical band gaps for the La, Pr, and Nd members were estimated to be 2.07, 2.09, and 2.12 eV, respectively, (Figure 2b

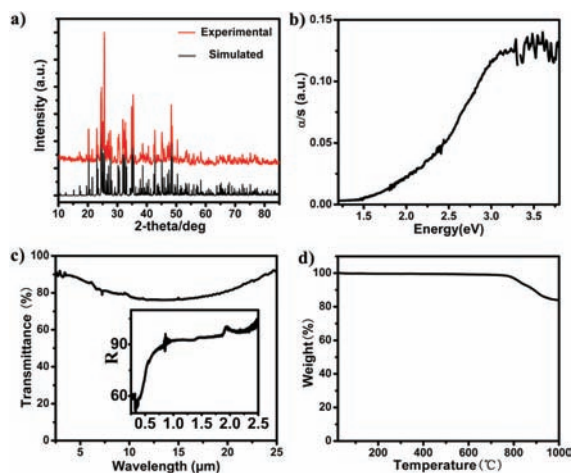


**Figure 2.** (a) Experimental and simulated X-ray diffraction patterns, (b) UV/vis/NIR diffuse reflectance spectrum, (c) IR and (inset) UV/vis/NIR transmittance curves, and (d) thermogravimetric analysis curve for  $\text{La}_4\text{InSbS}_9$ .

and Figure S7), which are comparable to that of commercial  $\text{AgGaS}_2$  (2.62 eV),<sup>10</sup> implying that  $\text{La}_4\text{InSbS}_9$  may have a suitable laser damage threshold for NLO applications. Several  $\text{Nd}^{3+}$  characteristic f–f transition absorptions between 1.3 and 2.1 eV were observed for  $\text{Nd}_4\text{InSbS}_9$ , similar to those for  $\text{NaNdGa}_4\text{Se}_8$ .<sup>11</sup> The diffuse-reflectance and IR spectroscopy

studies indicated that powdered  $\text{La}_4\text{InSbS}_9$  exhibits wide transparency comparable to that of powdered  $\text{AgGaS}_2$  [1.0–25  $\mu\text{m}$  (Figure 2c) vs 0.6–25  $\mu\text{m}$  (Figure S8)]. These data distinguish  $\text{La}_4\text{InSbS}_9$  as a potential candidate for NLO materials in the mid- and far-IR regions.

The electronic structures of  $\text{La}_4\text{InSbS}_9$  were investigated using DFT (Figure S9). The valence band (VB) maximum and conduction band (CB) minimum are located at different  $k$  points indicating an indirect band gap of 2.23 eV, which is close to the experimental value. As the total and partial density of states (DOS) (Figure S10) indicate, the top of the VB is dominated by S 3p states, whereas the bottom of the CB is primarily derived from La 5d states mixed with some Sb 5p and In 5s states. Thus, the band gap absorption is likely to be the result of electronic transitions from S 3p to La 5d states.

Remarkably,  $\text{La}_4\text{InSbS}_9$  displays an SHG intensity 1.5 times that of commercial  $\text{AgGaS}_2$  in an IR laser at 2.05  $\mu\text{m}$  (Figure

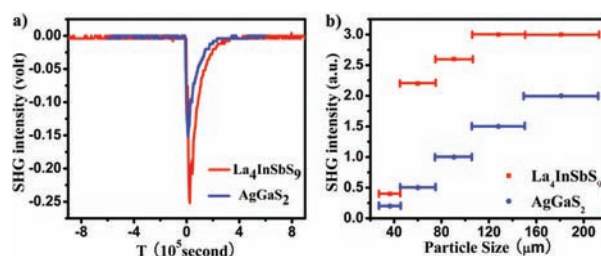


**Figure 3.** (a) Oscilloscope traces of the SHG signals of  $\text{La}_4\text{InSbS}_9$  and  $\text{AgGaS}_2$  at the same particle size of 150–210  $\mu\text{m}$ . (b) Particle-size dependence of the SHG intensity for  $\text{La}_4\text{InSbS}_9$  and  $\text{AgGaS}_2$ .

3). Moreover, the SHG intensities increase with the particle size and are saturated at a maximum value, indicating type-I phase-matchable behavior. No obvious SHG signals were observed for the Pr and Nd members, possibly because of their much poorer crystallinity.

At first sight, this nonzero SHG response of  $\text{La}_4\text{InSbS}_9$  is very surprising. As it crystallizes in space group  $P4_12_12$ , which belongs to the 422 point group, the space-group symmetry requires two nonvanishing tensors of second-order susceptibilities to follow the equation  $d_{14} = -d_{25}$ . On the other hand, under the restriction of Kleinman symmetry,<sup>1</sup>  $d_{14}$  must be equal to  $d_{25}$  (i.e.,  $d_{14} = d_{25}$ ). Consequently, both  $d_{14}$  and  $d_{25}$  must be equal to zero. Therefore, any material crystallizing in the 422 point group is forbidden from exhibiting an SHG response by Kleinman symmetry. Since Kleinman symmetry is based on the assumption that the medium is dispersionless, the presence of dispersion can damage its validity, leading to a very weak SHG response. For instance,  $\alpha\text{-TeO}_2$  exhibits a small  $d_{14}$  of  $\sim 0.36$  pm/V at 1.328  $\mu\text{m}$ .<sup>2a,h</sup> Electronic exciton resonance, which would be expected only when the second harmonic frequency is close to an absorption band gap of the material, can significantly enhance the SHG effect,<sup>12</sup> leading to strong violations of Kleinman symmetry.<sup>2a,h-1</sup> For instance,  $\alpha\text{-TeO}_2$ <sup>2a,i</sup> displays a large  $d_{14}$  value of 4.32 pm/V at 0.659  $\mu\text{m}$ , for which the second harmonic wavelength is 0.33  $\mu\text{m}$  ( $\sim 3.76$  eV), which is very close to its optical band gap (3.75 eV).<sup>2m</sup> However, this cannot explain the very large SHG coefficient of the title compound  $\text{La}_4\text{InSbS}_9$  under our measurement conditions (roughly estimated to be 20 pm/V, which is 5 times that of  $\alpha\text{-TeO}_2$ ). In this case, the second harmonic wavelength is  $\sim 1.00$   $\mu\text{m}$  ( $\sim 1.2$  eV), which differs significantly from the optical band gap (2.07 eV). Therefore, the electronic resonance

would not be expected. As a further confirmation of this, we first calculated the second-order NLO susceptibility coefficients of  $\text{La}_4\text{InSbS}_9$  using the length-gauge formalism derived by Aversa and Sipe, and null static SHG coefficients were then obtained to satisfy the Kleinman relations in the zero-frequency limit<sup>13</sup> (for details, see the SI). Consequently, the second-order NLO coefficients of some possible configurations of  $\text{La}_4\text{InSbS}_9$  were calculated. These configurations were obtained via ab initio MD simulations at 300 K using the Nosé algorithm (for details, see the SI). The structure simulation length was 10 ps with a time step of 1 fs. After 7 ps, 11 typical configurations were chosen. The calculation results are summarized in Table S4. Nine of the 11 configurations had NLO coefficients close to 15 pm/V, which roughly agrees with the experimental observation: 1.5 times that of  $\text{AgGaS}_2$  [i.e.,  $d_{36}(10.6 \mu\text{m}) = 13 \text{ pm/V}$ ].<sup>14</sup> These results strongly suggest that thermal vibrations of the lattice induce structure configurational variations that may be responsible for the strong SHG effect of  $\text{La}_4\text{InSbS}_9$ .

Meanwhile,  $\text{La}_4\text{InSbS}_9$  exhibits excellent thermal stability and shows no obvious weight loss up to 765 °C (Figure 2d and Figure S11). The 16% weight loss above 765 °C corresponds to the decomposition and the volatilization of  $\text{Sb}_2\text{S}_3$  (mp 550 °C) and is close to the calculated value of 15.7% (for details, see the SI).

In summary, three quaternary chiral chalcogenides with their own structure type,  $\text{Ln}_4\text{InSbS}_9 \equiv (\text{Ln}^{3+})_8([\text{In}_2\text{Sb}_2\text{S}_{11}]^{10-})(\text{S}^{2-})_7$  (Ln = La, Pr, Nd) have been reported. The major structure motif is  $[\text{In}_2\text{Sb}_2\text{S}_{11}^{10-}]_\infty$  infinite helical chains propagating along the  $c$  direction that are well-separated by  $\text{Ln}^{3+}$  cations and discrete  $\text{S}^{2-}$  anions. Remarkably, the La member shows the strongest Kleinman-forbidden SHG effects to date, with an intensity 1.5 times that of the commercial IR NLO material  $\text{AgGaS}_2$  under type-I phase-matching conditions at a laser wavelength of 2.05  $\mu\text{m}$ . Meanwhile, the powdered La member exhibits a band gap of 2.07 eV, high transparency (1.00–25.00  $\mu\text{m}$ ), and excellent thermal stability up to 765 °C. These primary data indicate that  $\text{La}_4\text{InSbS}_9$  is a potential candidate for IR NLO applications. The theoretical studies suggest that the origin and magnitude of the strong SHG response may originate from thermal vibrations of the lattice.

## ■ ASSOCIATED CONTENT

### ■ Supporting Information

Crystallographic data (CIF), experimental and theoretical methods, and additional tables and figures. This material is available free of charge via the Internet at <http://pubs.acs.org>.

## ■ AUTHOR INFORMATION

### Corresponding Author

chenl@fjirsm.ac.cn

## ■ ACKNOWLEDGMENTS

This research was supported by the National Natural Science Foundation of China (Projects 90922021, 21171168, and 90922022), the Knowledge Innovation Program of the Chinese Academy of Sciences (KJCX2-YW-H20), and the NSF of Fujian Province (2011J05039). We thank Prof. Ning Ye and Dr. Xin-Song Lin at FJIRSM for help with the SHG measurements.

## ■ REFERENCES

- (1) Kleinman, D. A. *Phys. Rev.* **1962**, *126*, 1977.
- (2) (a) Levine, B. F. *IEEE J. Quantum Electron.* **1973**, *QE-9*, 946. (b) Singh, S.; Bonner, W. A.; Van Uitert, L. G. *Phys. Lett.* **1972**, *38A*, 407. (c) Chemla, D. S.; Jerphagnon, J. *Appl. Phys. Lett.* **1972**, *20*, 222. (d) Porter, Y.; Halasyamani, P. S. *Chem. Mater.* **2001**, *13*, 1910. (e) Guo, S.-P.; Guo, G.-C.; Wang, M.-S.; Zou, J.-P.; Zeng, H.-Y.; Cai, L.-Z.; Huang, J.-S. *Chem. Commun.* **2009**, 4366. (f) Crane, G. R.; Bergman, J. G. *J. Chem. Phys.* **1976**, *64*, 27. (g) Okada, M.; Ieiri, S. *Phys. Lett.* **1971**, *34A*, 63. (h) Franken, P. A.; Ward, J. F. *Rev. Mod. Phys.* **1963**, *35*, 23. (i) Levine, B. F.; Miller, R. C. *Phys. Rev. B* **1975**, *12*, 4512. (j) Dailey, C. A.; Burke, B. J.; Simpson, G. J. *Chem. Phys. Lett.* **2004**, *390*, 8. (k) Xu, M. Z.; Jiang, S. D. *J. Phys.: Condens. Matter* **2006**, *18*, 8987. (l) Berkaine, N.; Orhan, E.; Masson, O.; Thomas, P.; Junquera, J. *Phys. Rev. B* **2011**, *83*, No. 245205. (m) Al-Kuhaili, M. F.; Durrani, S. M. A.; Khawaja, E. E.; Shirokoff, J. J. *Phys. D: Appl. Phys.* **2002**, *35*, 910.
- (3) (a) Halasyamani, P. S.; Poeppelmeier, K. R. *Chem. Mater.* **1998**, *10*, 2753. (b) Ra, H.-S.; Ok, K.-M.; Halasyamani, P. S. *J. Am. Chem. Soc.* **2003**, *125*, 7764. (c) Bera, T. K.; Jang, J. I.; Song, J.-H.; Malliakas, C. D.; Freeman, A. J.; Ketterson, J. B.; Kanatzidis, M. G. *J. Am. Chem. Soc.* **2010**, *132*, 3484. (d) Gandrud, W. B.; Boyd, G. D.; McFee, J. H. N. *Appl. Phys. Lett.* **1970**, *16*, 59. (e) Zhang, Q.; Chung, I.; Jang, J. I.; Ketterson, J. B.; Kanatzidis, M. G. *J. Am. Chem. Soc.* **2009**, *131*, 9896.
- (4) (a) Chen, M.-C.; Li, L.-H.; Chen, Y.-B.; Chen, L. *J. Am. Chem. Soc.* **2011**, *133*, 4617. (b) Zhao, H.-J.; Li, L.-H.; Wu, L.-M.; Chen, L. *Inorg. Chem.* **2009**, *48*, 11518. (c) Zhao, H.-J.; Li, L.-H.; Wu, L.-M.; Chen, L. *Inorg. Chem.* **2010**, *49*, 5811.
- (5) Assoud, A.; Kleinke, K. M.; Kleinke, H. *Chem. Mater.* **2006**, *18*, 1041.
- (6) Hahn, H.; Frank, G.; Klingler, W.; Meyer, A. D.; Stoerger, G. Z. *Anorg. Allg. Chem.* **1953**, *271*, 153.
- (7) Mauricot, R.; Gressier, P.; Evain, M.; Brec, R. *J. Alloys Compd.* **1995**, *223*, 130.
- (8) Sleight, A. W.; Prewitt, C. T. *Inorg. Chem.* **1968**, *7*, 2282.
- (9) West, A. R. *Solid State Chemistry and Its Applications*; Wiley: Chichester, U.K., 1984.
- (10) (a) Chemla, D. S.; Kupecek, P. J.; Robertson, D. S.; Smith, R. C. *Opt. Commun.* **1971**, *3*, 29. (b) Boyd, G. D.; Kasper, H.; McFee, J. M. *IEEE J. Quantum Electron.* **1971**, *QE-7*, 563. (c) Bhar, G. C.; Smith, R. C. *Phys. Status Solidi A* **1972**, *13*, 157.
- (11) Choudhury, A.; Dorhout, P. K. *Inorg. Chem.* **2008**, *47*, 3603.
- (12) (a) Wynne, J. J. *Phys. Rev. Lett.* **1971**, *27*, 17. (b) Zhang, X.-Q.; Tang, Z.-K.; Kawasaki, M.; Ohtomo, A.; Koinuma, H. *J. Phys.: Condens. Matter.* **2003**, *15*, 5191.
- (13) Rashkeev, S. N.; Lambrecht, W. R. L. *Phys. Rev. B* **2001**, *63*, No. 165212.
- (14) Dmitriev, V. G.; Gurzadyan, G. G.; Nikogosyan, D. N. *Handbook of Nonlinear Optical Crystals*, 3rd ed.; Springer: New York, 1999.